The EMBO Journal (2007) 26, 668–677 | © 2007 European Molecular Biology Organization | All Rights Reserved 0261-4189/07
www.embojournal.org

THE EMBO JOURNAL

A MAPK docking site is critical for downregulation of Capicua by Torso and EGFR RTK signaling

Sergio Astigarraga[1], Rona Grossman[2], Julieta Díaz-Delfín[3], Carme Caelles[3], Ze'ev Paroush[2] and Gerardo Jiménez[1,4,*]

[1]Institut de Biologia Molecular de Barcelona-CSIC, Parc Científic de Barcelona, Barcelona, Spain, [2]Department of Biochemistry, Faculty of Medicine, The Hebrew University, Jerusalem, Israel, [3]Institut de Recerca Biomèdica, Parc Científic de Barcelona, Barcelona, Spain and [4]Institució Catalana de Recerca i Estudis Avançats (ICREA), Barcelona, Spain

Early *Drosophila* development requires two receptor tyrosine kinase (RTK) pathways: the Torso and the Epidermal growth factor receptor (EGFR) pathways, which regulate terminal and dorsal-ventral patterning, respectively. Previous studies have shown that these pathways, either directly or indirectly, lead to post-transcriptional downregulation of the Capicua repressor in the early embryo and in the ovary. Here, we show that both regulatory effects are direct and depend on a MAPK docking site in Capicua that physically interacts with the MAPK Rolled. Capicua derivatives lacking this docking site cause dominant phenotypes similar to those resulting from loss of Torso and EGFR activities. Such phenotypes arise from inappropriate repression of genes normally expressed in response to Torso and EGFR signaling. Our results are consistent with a model whereby Capicua is the main nuclear effector of the Torso pathway, but only one of different effectors responding to EGFR signaling. Finally, we describe differences in the modes of Capicua downregulation by Torso and EGFR signaling, raising the possibility that such differences contribute to the tissue specificity of both signals.

The EMBO Journal (2006) **26,** 668–677. doi:10.1038/sj.emboj.7601532; Published online 25 January 2007
Subject Categories: signal transduction; development
Keywords: Capicua; *Drosophila*; oogenesis; RTK signaling; terminal patterning

Introduction

Receptor tyrosine kinases (RTKs) are a large family of cell surface receptors that translate extracellular signals into changes in gene expression and cellular function. Many RTKs signal through the evolutionarily conserved Ras/MAPK cassette, in which a cascade of interacting kinases ultimately leads to phosphorylation of nuclear transcription factors. As essentially the same Ras/MAPK cassette is used in multiple developmental contexts, a fundamental question has been how Ras/MAPK signals are interpreted to produce tissue-specific outputs (Rommel and Hafen, 1998; Tan and Kim, 1999). Here, we investigate the responses of a single nuclear protein, Capicua, to two distinct RTK pathways during *Drosophila* development.

Patterning of the *Drosophila* embryo and its surrounding eggshell requires two different RTK pathways initiated by the transmembrane receptors Torso and Epidermal growth factor receptor (EGFR). The Torso pathway controls the specification of the most anterior and posterior (terminal) regions of the embryo (Duffy and Perrimon, 1994; Furriols and Casanova, 2003). An extracellular signal produced during oogenesis activates Torso at each pole of the blastoderm embryo, leading to stimulation of the Ras/MAPK pathway, and hence, to localized activation of the gap genes *tailless* (*tll*) and *huckebein* (*hkb*) in terminal positions (Pignoni *et al*, 1990; Brönner and Jäckle, 1991; Duffy and Perrimon, 1994; Furriols and Casanova, 2003). Although regulation of *tll* and *hkb* at the anterior pole is complex and requires additional inputs from the anterior and dorsal-ventral (DV) maternal systems (Pignoni *et al*, 1992; Brönner *et al*, 1994; Reuter and Leptin, 1994), the activation of *tll* and *hkb* at the posterior pole occurs mainly in response to the Torso pathway. This activation, however, is indirect and involves a mechanism of derepression: both genes are normally repressed in central regions of the embryo and the Torso signal counteracts this repression to permit localized *tll* and *hkb* transcription at the pole (Liaw *et al*, 1995; Paroush *et al*, 1997; Jiménez *et al*, 2000). Repression of *tll* and *hkb* requires several nuclear factors such as the high-mobility group (HMG) protein Capicua (Cic) and the Groucho (Gro) corepressor. Embryos lacking maternally contributed Cic or Gro show derepression of *tll* and *hkb* towards the center of the embryo, which then leads to suppression of the thoracic and abdominal primordia (Paroush *et al*, 1997; Jiménez *et al*, 2000). Cic has been proposed to be the target of the Torso inhibitory signal because the protein appears excluded from the embryo poles in a Torso-dependent manner (Jiménez *et al*, 2000). However, it is not known whether this exclusion is direct, nor whether it is essential for the interpretation of the Torso signal.

Earlier in development, EGFR signaling also appears to establish antagonistic interactions with Cic. The EGFR pathway patterns the DV axis of both the embryo and the eggshell (Ray and Schüpbach, 1996). During mid-oogenesis (stage 9), the Gurken ligand is secreted at the dorsal-anterior corner of the oocyte and activates the EGFR present in the adjacent somatic follicle cells, thus conferring to these cells a dorsal fate. Subsequently, the dorsal-anterior follicle cells secrete the dorsal respiratory appendages of the eggshell, whereas the ventral follicle cells produce an extracellular signal towards the oocyte that will specify the ventral regions of the embryo. Mutations that prevent EGFR signaling lead to ventralization of the eggshell and the embryo, whereas ectopic EGFR

*Corresponding author. Department of Molecular and Cellular Biology, Institut de Biologia Molecular de Barcelona-CSIC, Parc Cientific de Barcelona, Josep Samitier, 1-5, Barcelona 08028, Spain.
Tel.: +34 934 034 970; Fax: +34 934 034 979;
E-mail: gjcbmc@ibmb.csic.es

Received: 8 June 2006; accepted: 7 December 2006; published online: 25 January 2007

activation dorsalizes the egg (Schüpbach, 1987; Queenan *et al*, 1997). Dorsalization phenotypes are also produced by several *cic* loss-of-function alleles, indicating that Cic normally prevents ventral and lateral follicle cells from acquiring a dorsal fate (Goff *et al*, 2001; Atkey *et al*, 2006). Additionally, Cic has been reported to accumulate in the nucleus of follicle cells except in dorsal-anterior regions, where EGFR is active (Goff *et al*, 2001). Again, the functional importance of this exclusion remains untested.

In this paper, we show that Cic is a direct nuclear target of the Torso and EGFR pathways. We identify a critical regulatory motif in Cic (designated C2) that functions as a MAPK docking site and interacts with Rolled, the MAPK acting in the Torso and EGFR pathways (Biggs and Zipursky, 1992; Biggs *et al*, 1994; Brunner *et al*, 1994). Mutations in the C2 motif generate Cic derivatives that escape downregulation by Torso and EGFR signaling and produce phenotypes that resemble those resulting from the loss of Torso and EGFR function. These results indicate that Cic downregulation is essential for both terminal and DV patterning. We also describe differences in the modes of Cic downregulation by Torso and EGFR signaling and discuss the possible mechanisms underlying those Cic responses.

Results

Independent motifs in Cic mediate transcriptional repression and downregulation by Torso

We first sought to identify the domains required for Cic repressor activity and for downregulation by Torso. Cic orthologs from invertebrate and vertebrate species share two well-conserved regions: the HMG-box presumed to mediate binding to target promoters and a C-terminal domain of unknown function (Jiménez *et al*, 2000; Figure 1A). To test if these two regions might suffice to provide Cic function, we designed a mini-Cic derivative (Cic^{mini}) containing both regions, but lacking most of the remaining non-conserved sequences (Figure 1B). The Cic^{mini} construct was tagged with the hemaglutinin (HA) epitope, placed under the control of *cic* genomic sequences and transformed into flies (Materials and methods). Maternal expression of Cic^{mini} rescues the phenotypes caused by the cic^{1} mutation (Figure 1C–E; Jiménez *et al*, 2000). This indicates that Cic^{mini} is able to repress *tll* and *hkb* in the central regions of the embryo. Furthermore, Cic^{mini} accumulates efficiently in the embryo, but is clearly absent from the poles (Figure 1G and H), suggesting that it also responds to Torso-mediated downregulation. Thus, the critical domains mediating Cic activity and regulation are contained within the Cic^{mini} construct.

Next, we assayed the effects of mutating the conserved domains of Cic. We first tested a Cic derivative lacking the HMG domain ($Cic^{\Delta HMG}$; Figure 1B). Expression of $Cic^{\Delta HMG}$ fails to rescue cic^{1} embryos (data not shown), demonstrating the requirement of the HMG domain for Cic function. Moreover, $Cic^{\Delta HMG}$ localizes predominantly in the cytoplasm of blastoderm embryos (Figure 1I), suggesting that the HMG region contains nuclear localization signals (NLSs) that target Cic to the nucleus. This cytoplasmic localization of $Cic^{\Delta HMG}$ is not the sole cause underlying its lack of rescuing activity, as an additional derivative (designated $Cic^{miniNLS}$; Figure 1B), in which the HMG domain of Cic^{mini} was replaced by the NLS from SV40 T antigen (Kalderon *et al*, 1984), is unable to rescue the cic^{1} mutant phenotype despite being nuclear (Figure 1B and J; data not shown). Thus, the HMG domain has additional roles other than mediating nuclear localization, most probably the binding to regulatory DNA sequences in target genes. We also find that $Cic^{\Delta HMG}$ is clearly detectable at the embryonic poles, suggesting that it is insensitive to downregulation by Torso signaling (Figure 1I). This could indicate that Cic downregulation requires access of the

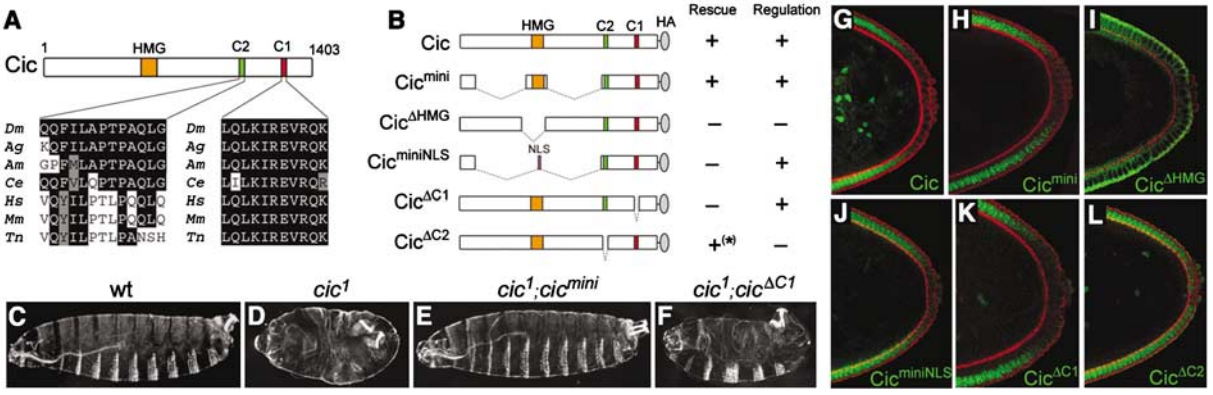

Figure 1 Different motifs in Cic mediate repressor function and downregulation by Torso. (**A**) Diagram of Cic protein and evolutionary conservation of the C1 and C2 motifs. The *Drosophila* sequences shown correspond to residues 1345–1355 (C1) and 1052–1071 (C2); the total length of Cic is 1403 amino acids. Identical and similar residues are boxed in black and gray, respectively. *Ag*, *Anopheles gambiae*; *Am*, *Apis mellifera*; *Ce*, *Caenorhabditis elegans*; *Hs*, *Homo sapiens*; *Mm*, *Mus musculus*; *Tn*, *Tetraodon nigroviridis*. The distantly related C2-like sequences from vertebrate orthologs are present in approximately equivalent positions between the HMG box and the C-terminus of those proteins. (**B**) Diagram of Cic derivatives expressed under the control of *cic* regulatory sequences. The HA tag is represented by a gray oval. The rescue activities and regulation of each construct are indicated on the right. The rescue activity of $Cic^{\Delta C2}$ was assayed using weak $cic^{\Delta C2}$ insertions that do not cause embryonic lethality in one copy (asterisk). (**C**) Embryonic cuticle of wild-type embryo. (**D**) cic^{1} mutant embryo with strongly suppressed trunk and abdomen. (**E**) cic^{1} mutant embryo rescued by maternal expression of Cic^{mini}. (**F**) cic^{1} embryo showing only partial rescue by $Cic^{\Delta C1}$. (G–L) Distribution of different Cic derivatives at the posterior of blastoderm embryos. Embryos were stained with anti-HA antibody (green) and rhodamine–phalloidin (red) to visualize the cortical actin associated with the plasma membrane. Wild-type Cic (**G**), Cic^{mini} (**H**), $Cic^{miniNLS}$ (**J**) and $Cic^{\Delta C1}$ (**K**) proteins exhibit significant downregulation at the pole. In contrast, $Cic^{\Delta C2}$ accumulates ectopically at the pole and in germ cells (**L**). Note the cytoplasmic localization of $Cic^{\Delta HMG}$ and its accumulation at the pole (**I**). Identical results were obtained at the anterior of the embryo (Supplementary Figure 1 and data not shown).

protein to the nucleus, or that the HMG domain is directly involved in the mechanism of Cic downregulation. In support of the first possibility, the nuclear Cic^{miniNLS} derivative displays significant downregulation at the poles in the absence of a functional HMG domain (Figure 1J).

We distinguish two conserved motifs within the C-terminal region of Cic, which we designate as C1 and C2. C1 is a 48-amino-acid sequence containing a highly invariable core of 11 residues present in all Cic orthologs (Figure 1A; Jiménez *et al*, 2000). We find that a C1-deleted derivative (Cic$^{\Delta C1}$; Figure 1B) produces only partial rescue of *cic*^{1} mutant embryos (Figure 1F). This suggests that the C1 motif is important for Cic repressor activity. In contrast, this motif is dispensable for Torso-dependent regulation because Cic$^{\Delta C1}$ is clearly suppressed at the embryo poles (Figure 1K).

The C2 motif is highly conserved in Cic orthologs from insects and nematodes, but appears to have diverged in vertebrate Cic proteins (Figure 1A). We find that the expression of a Cic derivative carrying a deletion of C2 (Cic$^{\Delta C2}$; Figure 1B) has a strong maternal effect, resulting in embryonic lethality. The penetrance of this effect is >95% with a single copy of the transgene in approximately half of the transgenic lines (data not shown). The remaining lines cause embryonic lethality only when two copies are present. A single copy of weak *cic*$^{\Delta C2}$ insertions rescues the *cic*^{1} mutation to adulthood (data not shown), indicating that Cic$^{\Delta C2}$ is a functional repressor. Remarkably, Cic$^{\Delta C2}$ accumulates extensively at the embryo poles and in pole cell nuclei (Figure 1L and Supplementary Figure 1). This ectopic accumulation of Cic$^{\Delta C2}$ is also observed in *cic*^{1} mutant embryos that lack endogenous Cic protein (data not shown), suggesting that this result does not simply reflect saturation of the downregulation machinery by the combined expression of Cic$^{\Delta C2}$ and endogenous Cic. Thus, the C2 motif is specifically required for Cic downregulation in response to Torso signaling.

Embryos expressing strong *cic*$^{\Delta C2}$ insertions frequently lack the eighth abdominal segment and the posterior spiracle (Figure 2A), a phenotype shared by mutants lacking Torso activity (Duffy and Perrimon, 1994). Stronger defects extending to the abdominal region are also observed in approximately 40% of the embryos (Figure 2B). We hypothesized that Cic$^{\Delta C2}$ is a dominant repressor that escapes downregulation by Torso and consequently perturbs posterior terminal development. Indeed, *cic*$^{\Delta C2}$ embryos exhibit reduced or absent posterior expression of *tll* and *hkb* (Figure 2C–F), indicating that Cic$^{\Delta C2}$ represses both genes even in terminal nuclei exposed to Torso activity. We also examined the expression of *hunchback* (*hb*), which normally forms a posterior stripe under the control of *tll* and *hkb* function (Casanova, 1990; Brönner and Jäckle, 1991; Figure 2G). As shown in Figure 2H, this *hb* stripe is shifted towards the pole in *cic*$^{\Delta C2}$ embryos, again indicating that Cic$^{\Delta C2}$ interferes with posterior terminal patterning. In contrast, the effects of Cic$^{\Delta C2}$ are much weaker at the anterior pole, resulting in reduced *hkb* expression and mildly affected patterns of *tll* and *hb* (Figure 2C–H; see Discussion). We conclude that Cic downregulation is essential for the correct specification of posterior terminal structures and critically depends on the C2 motif.

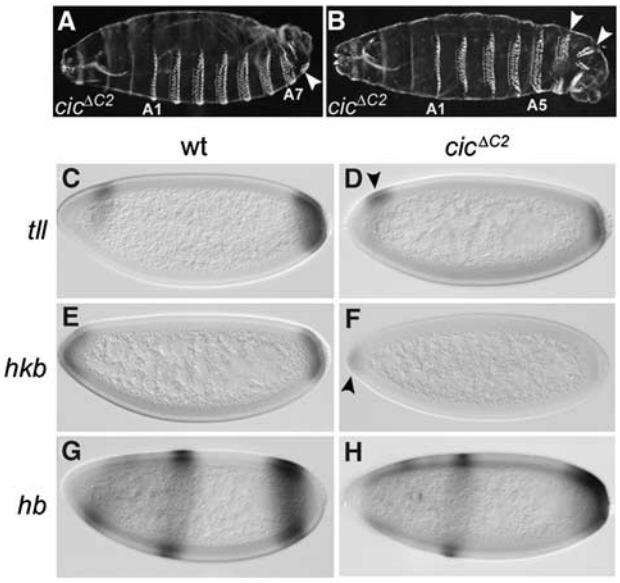

Figure 2 Cic$^{\Delta C2}$ interferes with embryonic terminal development. (**A, B**) Cuticle phenotypes resulting from maternal expression of Cic$^{\Delta C2}$. Shown are examples of intermediate phenotypes characterized by the lack of posterior terminal structures including the A8 segment (A, arrowhead), and stronger effects where additional segments (typically A6 and A7, arrowheads) are affected (B). (C–H) mRNA expression patterns of *tll* (**C, D**), *hkb* (**E, F**) and *hb* (**G, H**) in wild-type (C, E, G) and *cic*$^{\Delta C2}$ (D, F, H) embryos. The mutant embryos exhibit marked repression of *tll* and *hkb* at the posterior pole, and shifted expression of the posterior *hb* stripe. At the anterior region, *hkb* expression appears markedly reduced (arrowhead in F). We also note a slight anterior shift (of approximately 6% egg length) of the dorsal *tll* stripe (arrowhead in D).

The C2 motif is a MAPK docking site

The C2 element contains a TP dipeptide (amino acids 1059–1060 in Cic; Figure 1A) that could be a potential MAPK phosphorylation site in response to Torso signaling. To test if phosphorylation of T1059 mediates downregulation of Cic, we generated Cic derivatives in which T1059 was replaced by either A or D residues that should prevent or mimic phosphorylation of this site, respectively. If phosphorylation of T1059 controls Cic downregulation, the T1059A mutation should be refractory and therefore more disruptive to this downregulation than T1059D. We, however, find that T1059D causes stronger suppression of Cic regulation than T1059A, suggesting that phosphorylation of T1059 is unlikely to explain the function of the C2 motif (Supplementary Figure 2).

We then tested the possibility that the C2 motif functions as a MAPK docking site for Rolled (Tanoue and Nishida, 2003). Using the yeast two-hybrid system we found that, indeed, a Cic fragment comprising the C1 and C2 motifs interacts strongly with Rolled (data not shown). Further experiments showed that the binding maps precisely to the C2 element (Figure 3A and B). The binding requires the C-terminus of Rolled (Figure 3B), which spans the common docking (CD) domain mediating association of MAPKs to their substrates (Tanoue *et al*, 2000). The C2 motif also interacts with the human Erk2 MAPK (Figure 3B). We independently confirmed the association between the C2 motif and Rolled using *in vitro* pull-down assays. A Cic fragment containing the C2 motif interacts with Rolled, whereas the equivalent fragment lacking the C2 core does not (Figure 3A and C; see also Supplementary Figure 2F). Furthermore, the C2 element mediates phosphorylation of Cic by Erk2 *in vitro*: activated Erk2 immunopurified from HeLa cells efficiently phosphorylates a Cic fragment including the C2 motif, but not

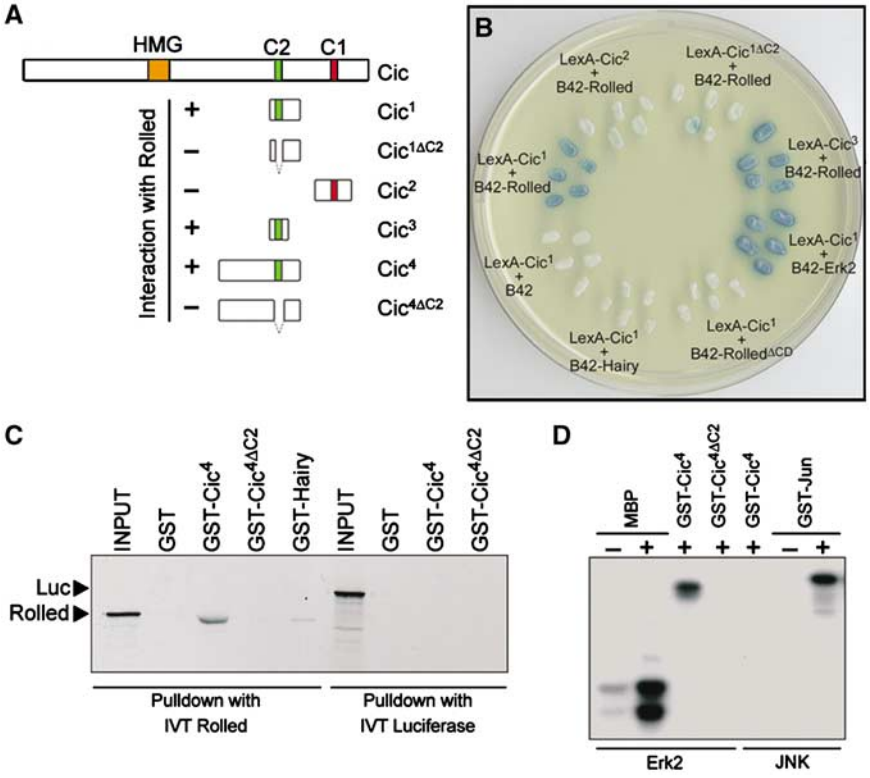

Figure 3 The C2 motif is a MAPK docking site. (**A**) Diagram of Cic protein showing the different fragments assayed for binding in yeast and *in vitro*. The limits of each Cic fragment are as follows: Cic^1 (1050–1115), Cic^2 (1307–1379), Cic^3 (1050–1079) and Cic^4 (942–1116). The C2 amino-acid sequences deleted in $Cic^{1\Delta C2}$ and $Cic^{4\Delta C2}$ are 1054–1064 and 1052–1072, respectively. (**B**) Yeast two-hybrid assay using different LexA-Cic baits and B42 fusion preys. Positive interactions (visualized by *lacZ* reporter activation) are observed between C2-containing fragments and Rolled or human Erk2. Negative controls are $Rolled^{\Delta CD}$, a form of Rolled lacking the C-terminal 52 amino acids that should be unable to bind substrates, and Hairy. (**C**) Pull-down assay using the indicated GST fusions and *in vitro* translated (IVT) Rolled or Luciferase (Luc) labeled with ^{35}S-methionine. Cic^4 binds Rolled in a C2-dependent manner. Negative controls show little or no interaction between Hairy and Rolled, or between Cic and Luciferase. Input lanes were loaded with 10% of the protein used in the binding reactions. (**D**) *In vitro* phosphorylation assay using the indicated GST fusions and either Erk2 or Jun kinase (JNK) protein immunopurified from HeLa cells unstimulated (−) or stimulated (+) for kinase activation. Positive control substrates for Erk2 and JNK were myelin basic protein (MBP) and Jun, respectively. Erk2 specifically phosphorylates Cic^4 but not $Cic^{4\Delta C2}$. The gels shown in (C) and (D) were stained with Coomassie to ensure equal loading and integrity of all GST fusions (not shown).

the equivalent C2-deleted fragment (Figure 3A and D). This phosphorylation is Erk2-specific because it is not observed while using activated Jun kinase (JNK; Figure 3D). Collectively, our results indicate that C2 is a docking motif that recruits Rolled to induce phosphorylation of Cic in response to signaling. Like other MAPK docking sites, the C2 element includes several conserved hydrophobic residues (Tanoue and Nishida, 2003), although their specific arrangement is different, suggesting that C2 represents a novel MAPK docking motif.

EGFR signaling alters the subcellular distribution of Cic in the ovary

We next investigated the regulation of Cic by EGFR signaling in the ovary. First, we re-examined the distribution of Cic in follicle cells using the sensitive HA-tagged version of the protein, which is able to rescue the *fettucine* (*fet*) alleles of *cic* that cause dorsalization of the egg (data not shown; Goff *et al*, 2001). In these experiments, we also monitored expression of *mirror*, an EGFR-induced target that marks the dorsal-anterior region of the egg chamber (Jordan *et al*, 2000; Zhao *et al*, 2000).

During stage 9–10A, Cic accumulates in the nuclei of follicle cells located outside the dorsal-anterior region (Figure 4A–D). Unexpectedly, we also detect Cic in dorsal-anterior cells, albeit equally distributed between the nucleus and the cytoplasm (Figure 4A–D; see also Supplementary Figure 3). This localization of epitope-tagged Cic was also observed in a cic^{fetU6}/cic^{fetE11} mutant background with reduced levels of endogenous Cic (data not shown), suggesting that accumulation of Cic in dorsal-anterior cells occurs at physiological levels of Cic expression. Later in oogenesis (stages 11–12), Cic regulation appears confined to a small patch of only ~40 dorsal follicle cells comprised within a broader area of Mirr expression (Figure 4E and F), suggesting that the domain of Cic downregulation has retracted towards the dorsal midline, whereas the Mirr expression domain has remained unaltered. Also, the late patch is divided by a stripe of cells in the presumptive midline in which Cic is preferentially nuclear (Figure 4F; empty arrowhead). This stripe coincides with the midline region in which EGFR signaling declines at this stage (Wasserman and Freeman, 1998; Peri *et al*, 1999; also see below). By stages 12–13, the patch of Cic regulation includes only 15–20 cells and the midline stripe of nuclear protein is still visible (data not shown). Thus, Cic regulation in follicle cells is dynamic and correlates with the evolving pattern of EGFR activity.

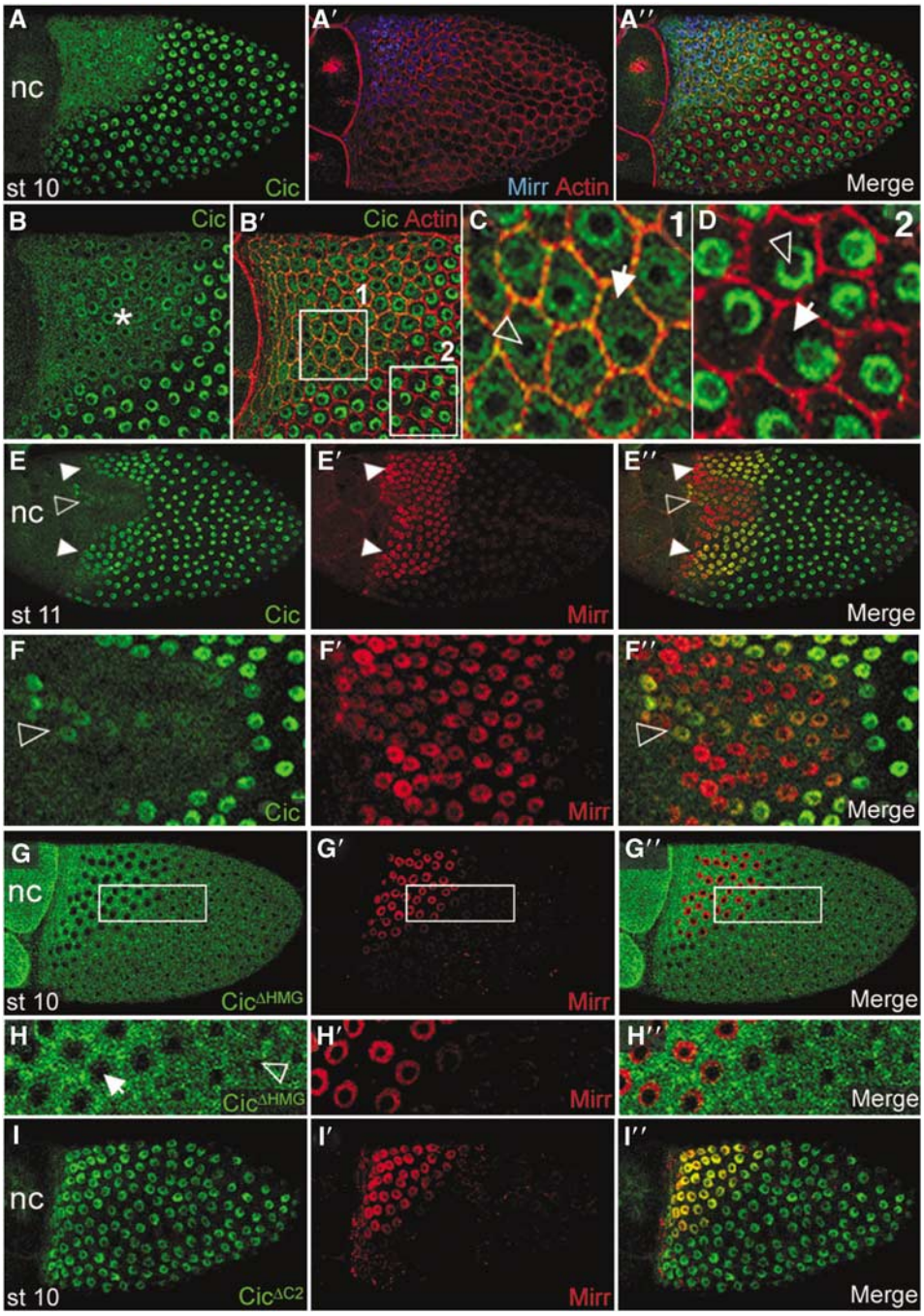

Figure 4 EGFR signaling induces nucleocytoplasmic redistribution of Cic via the C2 motif. (**A**) Partial view of a stage-10 *cic-HA* egg chamber costained with anti-HA (green, A) and anti-Mirror (Mirr; blue, **A′**) antibodies, and with rhodamine–phalloidin (red, A′) to label the cortical actin. The merged image is shown in (**A″**). (**B**) Detail of the dorsal-anterior region of the above egg chamber; expression of Mirr is not shown. The merged image is shown in (**B′**). The preferential nuclear accumulation of Cic in some cells (asterisk in B) probably results from regional differences in the levels of Ras/MAPK activation within the dorsal-anterior patch at this stage (Peri *et al*, 1999). (**C, D**) High magnifications of two areas from (B′) corresponding to dorsal-anterior (C, 1) and lateral (D, 2) follicle cells. Cic accumulates in the cytoplasm of dorsal-anterior but not lateral follicle cells (arrows). The central areas of nuclei devoid of staining probably correspond to nucleoli (empty arrowheads). (**E**) Dorsal view of a stage-11 *cic-HA* egg chamber stained with anti-HA (green, E) and anti-Mirr (red, **E′**) antibodies. The merged image is shown in (**E″**). Note the nuclear accumulation of Cic in cells that express Mirr (arrowheads) and the preferential nuclear accumulation of Cic in a row of cells in the presumptive midline (open arrowhead). (**F**) Detail of the dorsal-anterior region of the egg chamber shown in (E). (**G**) Partial view of a stage-10 $cic^{\Delta HMG}$*-HA* egg chamber stained as in (E). (**H**) Detail of the boxed area shown in (G). $Cic^{\Delta HMG}$ is excluded from the dorsal-anterior nuclei (arrow), whereas only the nucleoli remain devoid of protein in more posterior cells (open arrowhead). (**I**) Partial view of a stage-10 $cic^{\Delta C2}$*-HA* egg chamber stained as in (E). In the merge panels, colocalization of the green and red channels appears in yellow–orange, whereas colocalization of green and blue channels appears in cyan. Stages of egg chambers are indicated. nc, nurse cells.

We examined the localization of our Cic mutant derivatives in the ovary. Specifically, we find that $Cic^{\Delta HMG}$ accumulates in both the nucleus and cytoplasm of cells located outside the dorsal-anterior patch, and is exclusively cytoplasmic in this patch (Figure 4G and H). Moreover, the amount of cytoplasmic $Cic^{\Delta HMG}$ protein appears elevated in dorsal-anterior cells,

suggesting that Cic$^{\Delta HMG}$ becomes concentrated in the cytoplasm upon EGFR signaling and the total amount of protein in the cell remains unaltered. This result further indicates that Cic regulation in the ovary occurs at the level of nucleocytoplasmic localization rather than through degradation. In contrast, Cic$^{\Delta C2}$ is exclusively nuclear in all follicle cells, including those at dorsal-anterior regions (Figure 4I). This indicates that redistribution of Cic in response to EGFR signaling depends on the C2 motif. Notably, nuclear Cic$^{\Delta C2}$ does not affect Mirr expression (Figure 4I″), suggesting that EGFR-induced activation of *mirr* is not just a consequence of Cic downregulation (see Discussion).

DV patterning defects induced by Cic$^{\Delta C2}$

Unregulated accumulation of Cic$^{\Delta C2}$ in the dorsal-anterior follicle cells causes DV patterning defects. Females expressing strong *cic$^{\Delta C2}$* combinations produce eggs with partial or complete fusions of their dorsal respiratory appendages (Figure 5A–C). These ventralization phenotypes resemble those arising from insufficient EGFR activity in dorsal-anterior follicle cells (Schüpbach, 1987), indicating that EGFR-mediated downregulation of Cic is essential for the correct patterning of the eggshell.

Although *cic$^{\Delta C2}$* embryos do not show marked signs of ventralization in their cuticles, they do display altered expression of early ventral and dorsal markers such as *twist* (*twi*) and *zerknüllt* (*zen*) (Rusch and Levine, 1996). In wild-type embryos, *twi* forms a band of expression on the ventral side (Figure 5D). In comparison, more than 70% of *cic$^{\Delta C2}$* embryos show expanded *twi* expression towards the dorsal side, particularly in posterior regions (Figure 5E). Additionally, the dorsal-specific expression of *zen* retracts in *cic$^{\Delta C2}$* embryos, being almost absent in dorsal-posterior positions (Figure 5F and G). Thus, *cic$^{\Delta C2}$* embryos are moderately ventralized, raising the possibility that downregulation of Cic by EGFR signaling during oogenesis is important for establishing the DV pattern of the embryo. It should be noted, however, that the reduced *zen* expression at or near the posterior pole of *cic$^{\Delta C2}$* embryos could also be a consequence of ectopic Cic$^{\Delta C2}$ repressor activity at this position, as we have previously proposed that Cic participates in dorsal-mediated repression of zygotic targets such as *zen* (Jiménez *et al*, 2000).

To further examine how Cic$^{\Delta C2}$ interferes with embryonic DV patterning, we determined its effects on *pipe* expression in the ovary. *pipe* encodes a sulfotransferase expressed in ventral follicle cells that initiates the specification of the embryonic DV pattern (Sen *et al*, 1998; Figure 6A). We find that most *cic$^{\Delta C2}$* egg chambers show moderate, but significant expansion of *pipe* expression towards the dorsal side (Figure 6B). This expansion is more evident in dorsal-posterior regions, where the limit of *pipe* expression is shifted anteriorly by about 3–5 cell diameters (arrowhead in Figure 6B). This result supports the idea that downregulation of Cic in response to EGFR activation makes a modest contribution to the establishment of embryonic DV polarity (see Discussion).

We also examined the expression of *rhomboid* (*rho*) and *argos*, two additional DV patterning genes, in *cic$^{\Delta C2}$* egg chambers (see also Supplementary Figure 4 for an analysis of their expression in the *cic^{fet}* mutant ovaries). *rho* is an EGFR target that plays a central role in DV axis formation (Ruohola-Baker *et al*, 1993). In wild-type egg chambers, *rho* expression is dynamic and resolves into two dorsal, L-shaped stripes by stage 10B (Figure 6C). In *cic$^{\Delta C2}$* egg chambers, these stripes appear repressed, such that only residual discontinuous expression is visible (Figure 6D). This indicates that Cic downregulation is required for the normal activation or resolution of *rho* expression in response to EGFR. We next monitored *argos* expression because of its requirement for

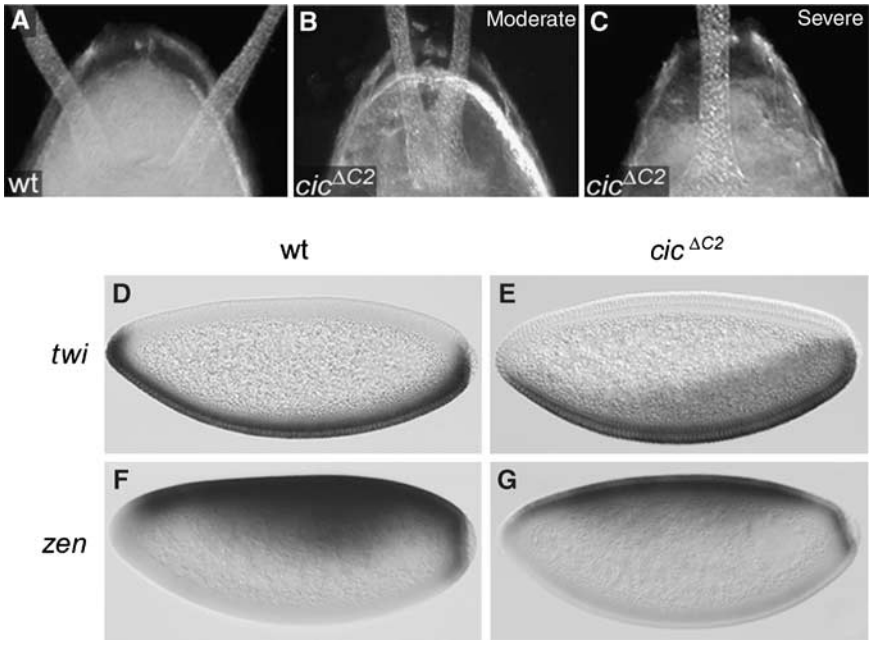

Figure 5 Cic$^{\Delta C2}$ causes DV patterning defects in the egg. (**A**) Dorsal-anterior region of a wild-type eggshell showing the two symmetrical respiratory appendages. (B, C) Equivalent views of *cic$^{\Delta C2}$* eggshells showing moderate (**B**) and severe (**C**) fusions of appendages. The frequencies of phenotypic classes resulting from strong *cic$^{\Delta C2}$* combinations are as follows: wild-type, 40%; moderate, 25%; severe, 30%. (D–G) mRNA expression patterns of *twi* (**D, E**) and *zen* (**F, G**) in wild-type (D, F) and *cic$^{\Delta C2}$* (E, G) embryos.

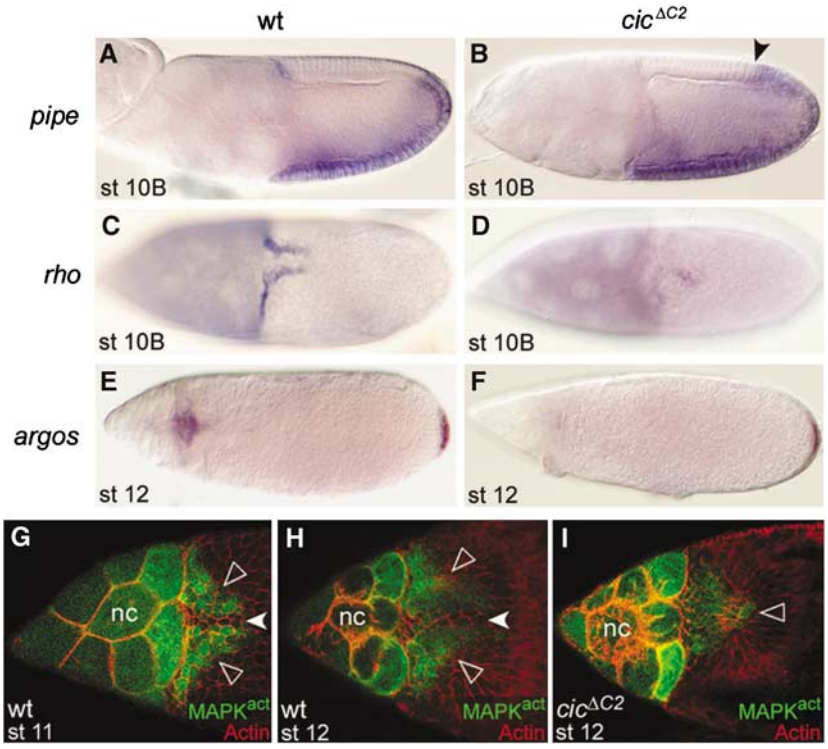

Figure 6 Cic$^{\Delta C2}$ interferes with the regulatory network controlling DV polarity in the ovary. (A–F) mRNA expression patterns of *pipe* (**A, B**), *rho* (**C, D**) and *argos* (**E, F**) in wild-type (A, C, E) and *cic*$^{\Delta C2}$ (B, D, F) egg chambers. Lateral views are shown in (A) and (B); dorsal views in (C–F). The *cic*$^{\Delta C2}$ egg chambers exhibit moderate expansion of *pipe* expression (arrowhead in panel B) and reduced or absent expression of both *rho* and *argos* in the dorsal-anterior region (panels D and F, respectively). Note that the expression of *argos* at the posterior end of the egg chamber is unaffected by Cic$^{\Delta C2}$ (F). (**G**) Dorsal view of a stage-11 wild-type egg chamber doubly stained for activated MAPK (MAPK^{act}, green) and actin (red). Two patches of activated MAPK (empty arrowheads) are separated by a row of cells devoid of staining (solid arrowhead). (H, I) Dorsal views of wild-type (**H**) and *cic*$^{\Delta C2}$ (**I**) egg chambers at stage 12 stained as in G. The two patches of activated MAPK staining appear fused in the mutant chamber (empty arrowhead in I). Stages of egg chambers are indicated. nc, nurse cells.

the correct separation of the two eggshell appendages (Wasserman and Freeman, 1998), a process that is disrupted by Cic$^{\Delta C2}$ expression (see above). Also, Cic acts as a negative regulator of *argos* during the specification of wing veins (Roch *et al*, 2002). In wild-type ovaries, *argos* is activated by EGFR signaling during stage 11, producing a T-shaped domain of expression centered on the dorsal midline (Figure 6E; Queenan *et al*, 1997; Wasserman and Freeman, 1998). The Argos product locally inhibits the EGFR signal and splits it into two dorsal-lateral domains, thereby specifying the two symmetrical appendages (Wasserman and Freeman, 1998). As shown in Figure 6F, most *cic*$^{\Delta C2}$ egg chambers fail to express *argos*, although we see residual staining in some chambers. Thus, EGFR-induced downregulation of Cic appears to be a necessary step for activation of *argos* and the subsequent division of EGFR signaling during late oogenesis.

This was further tested by examining the accumulation of activated MAPK in follicle cells. The splitting of EGFR signaling during stage 11 produces two symmetrical peaks of activated MAPK in the dorsal-anterior region (Wasserman and Freeman, 1998; Peri *et al*, 1999). These peaks are separated by a single row of cells devoid of staining from stage 11 through 13 (Figure 6G and H), which presumably corresponds to the midline stripe of nuclear Cic protein observed at that stage (Figure 4E and F). Significantly, in *cic*$^{\Delta C2}$ egg chambers the domains of MAPK activation appear partly or completely fused (Figure 6I), supporting an essential role for Cic downregulation in the transition from one to two peaks of EGFR signaling during eggshell patterning.

Discussion

The Torso and EGFR pathways regulate distinct aspects of early *Drosophila* development, such as the specification of embryonic terminal structures (Torso) and the establishment of DV polarity for both the embryo and the eggshell (EGFR). In this paper, we present evidence that both pathways exert their function, at least in part, by directly downregulating the Cic protein, and that these regulatory effects require a MAPK docking site in Cic (the C2 motif) that interacts with the MAPK Rolled. Below, we discuss the implications of these results for the role of Cic in terminal and DV patterning.

Inactivation of Cic by Torso signaling

Our results show that Cic is a direct nuclear effector of the Torso pathway, particularly in the posterior end of the embryo (see below). Furthermore, as Cic$^{\Delta C2}$ substantially blocks posterior terminal gene expression and differentiation, we infer that the other components of *tll* and *hkb* repression (e.g. Gro; Paroush *et al*, 1997) must be active at the pole to assist repression by Cic$^{\Delta C2}$. This suggests that Cic is the main, if not the only, target of the Torso pathway at the posterior. Although Cic$^{\Delta C2}$ does not fully suppress *tll* expression at the posterior pole (Figure 2D), our interpretation of this result is that Cic$^{\Delta C2}$ still retains residual downregulation and its ectopic accumulation at the pole does not reach the levels found in more central regions (Figure 1L), thus permitting weak *tll* transcription. In this regard, we note that downregulation of Cic^{mini} is less effective than that of wild-type Cic

(cf. Figure 1G and H), suggesting that in addition to the C2 motif, other Cic sequences may also contribute to its downregulation. It is also possible that full donwregulation of Cic requires input from a non-RTK pathway such as the posterior system (Cinnamon *et al*, 2004).

Combined with previous studies, our results suggest a model for the translation of the morphogenetic gradient of Torso activation into nested patterns of *tll* and *hkb* expression at the posterior (see Greenwood and Struhl, 1997; Paroush *et al*, 1997). The graded activity of Torso (with peak levels at the tip) creates a complementary gradient of Cic repressor activity. Cic then represses *tll* and *hkb* with different efficiencies such that *tll* repression requires a higher concentration of active Cic protein. This is consistent with the different sensitivities of *tll* and *hkb* to $Cic^{\Delta C2}$, and with our observation that low levels of wild-type Cic protein in subterminal positions overlap with the domain of *tll*, but not *hkb*, expression (unpublished work). In contrast, the output of the Torso pathway is more complex at the anterior pole. The effects of $Cic^{\Delta C2}$ on *hkb* anterior expression resemble those caused by loss of Torso pathway activity (Brönner and Jäckle, 1991; Reuter and Leptin, 1994), indicating that Cic downregulation in response to Torso signaling is important for the correct activation of *hkb* at the anterior. However, other aspects of Torso-mediated regulation, such as the retraction of *tll* and *hb* anterior expression, remain largely unaffected in $cic^{\Delta C2}$ embryos, indicating that they involve other sensors of the pathway. Indeed, several studies have demonstrated a direct downregulation of Bicoid transcriptional activity by Torso signaling at the anterior (Ronchi *et al*, 1993; Janody *et al*, 2001).

Downregulation of Cic by EGFR signaling in the ovary

We find that EGFR signaling induces intracellular relocalization of Cic in dorsal-anterior follicle cells. This relocalization is essential for the normal patterning of the eggshell and, to a lesser extent, of the embryo, given that unregulated $Cic^{\Delta C2}$ accumulation interferes with these processes. We presume that EGFR signaling downregulates Cic activity by reducing nuclear Cic levels below a critical threshold, although it is also possible that residual nuclear Cic protein in responding cells is inactive as a result of phosphorylation. In this regard, it has been shown that MAPK-related phosphorylation of the HMG-box protein TCF-4 inhibits its ability to form complexes with DNA and regulate transcription (Ishitani *et al*, 1999).

By analogy to the role of Cic in terminal patterning, the regulation of Cic by EGFR signaling during oogenesis might represent a mechanism of derepression. Our results indicate that Cic behaves as a repressor of *rho* and *argos* (Figure 6 and Supplementary Figure 4), raising the possibility that these genes are activated by the EGFR pathway, at least in part, through relief of Cic repression. A similar derepression mechanism has been proposed to explain how Cic controls *mirr* expression (Atkey *et al*, 2006; also see below). Nevertheless, it is possible that these interactions are indirect. For example, ectopic *rho* expression in *cic* mutant ovaries could be a consequence of derepression of *mirr* in those ovaries (Goff *et al*, 2001; Atkey *et al*, 2006), as ectopic *mirr* expression has been shown to activate *rho* (Jordan *et al*, 2000). Also, it is currently unknown whether Cic exerts a direct or indirect function as an activator of *pipe* expression (Goff *et al*, 2001).

Our results are consistent with a model where Cic is only one of several effectors regulated by the EGFR signal. Thus, the effects of $Cic^{\Delta C2}$ on embryonic DV patterning are considerably weaker than those caused by the loss of EGFR function. For example, $Cic^{\Delta C2}$ induces minor changes in *pipe* expression in the ovary (Figure 6B), whereas loss of EGFR activity causes a complete expansion of *pipe* expression towards the dorsal side (Sen *et al*, 1998). In addition, $Cic^{\Delta C2}$ does not prevent *mirr* expression in dorsal cells (Figure 4I), indicating that EGFR-dependent activation of this gene does not rely exclusively on Cic downregulation. This is also consistent with the finding that ectopic *mirr* expression in *cic* mutant ovaries appears weaker than in dorsal cells receiving the EGFR signal (Atkey *et al*, 2006). Similarly, Cic cannot be the only nuclear factor controlling the limits of *rho* and *argos* expression, because their patterns of expression are not simply complementary to the area of Cic distribution, and loss of Cic function causes only low-level ectopic expression of both genes in lateral and ventral follicle cells (Supplementary Figure 4). Finally, the EGFR pathway is known to target at least another nuclear factor, CF2, in follicle cells (Mantrova and Hsu, 1998; Hsu *et al*, 2001). Like Cic, CF2 acts as a suppressor of dorsal cell fates and, directly or indirectly, represses *rho* expression (Hsu *et al*, 1996). Interestingly, CF2 lacks a C2-like element and is predominantly degraded (rather than redistributed) in response to EGFR activation, suggesting that EGFR signaling relies on different mechanisms for targeting Cic and CF2.

Mechanisms of Cic downregulation

We know little about the mechanisms mediating degradation or subcellular redistribution of Cic in response to the Torso and EGFR signals, respectively. In the case of Torso signaling, our analyses of Cic derivatives lacking the HMG domain imply the existence of at least one nuclear step in the degradation of Cic at the embryo poles. Because Torso signaling induces accumulation of activated MAPK predominantly in the nucleus (our unpublished observations), we presume that one such nuclear step is the direct phosphorylation of Cic by the MAPK Rolled. Phosphorylated Cic could then be rapidly ubiquitinated and degraded by the proteasome, either within the nucleus or in the cytoplasm, after a nuclear export event. In the ovary, $Cic^{\Delta HMG}$ undergoes a marked cytoplasmic shift in dorsal-anterior follicle cells, implying the existence of an active mechanism of either nuclear export or cytoplasmic retention in response to EGFR signaling. Accordingly, the uniform intracellular distribution of wild-type Cic protein in dorsal-anterior cells does not seem to be a consequence of passive diffusion between nucleus and cytoplasm.

What might be the basis for the different modes of Cic downregulation in the embryo and in the ovary? Our finding that the C2 motif mediates both types of Cic regulation implies that they similarly arise from MAPK-induced phosphorylation. Thus, we favor the view that phosphorylated Cic undergoes degradation or redistribution as a result of intrinsic differences between the embryo and the follicle cells (see Simon, 2000), such as the lack of a critical degradation factor in the latter. Nevertheless, it is also conceivable that quantitative or qualitative differences in the sites of Cic phosphorylation influence the regulation of Cic in the two tissues. For example, different levels of MAPK-induced phosphorylation

of c-Fos are associated with changes in c-Fos stability and biological function (Murphy *et al*, 2002). However, quantitative differences in the graded activation of Torso at the embryo poles never result in detectable Cic protein in the embryonic cytoplasm (Figure 1G and Supplementary Figure 1A), suggesting that the two modes of Cic downregulation do not merely reflect different intensities of the Torso and EGFR signals.

Independent of the underlying mechanisms, the differential responses of Cic to Torso and EGFR signaling appear to correlate with distinct spatial-temporal profiles of the two signals. Whereas the Torso signal consists of a single, short signaling event, the EGFR signal is dynamic and involves sequential rounds of amplification and inhibition (Wasserman and Freeman, 1998). Perhaps the degradation of Cic in response to Torso represents a robust, irreversible mechanism of downregulation, whereas the subcellular redistribution of Cic induced by EGFR reflects a reversible response. In the latter case, dephosphorylation of Cic might allow a rapid relocalization of functional protein to the nucleus as the area of Cic regulation retracts during stages 11 and 12 of oogenesis. Future analyses will help define the different modes of Cic downregulation and the functional consequences associated with such differences.

Evolution of Cic regulation

The conservation of the C2 element in insects and nematodes suggests that Cic orthologs in these invertebrate species are responsive to RTK signals. In contrast, the C2 sequence is not well conserved in vertebrate Cic proteins (Figure 1A; see also Supplementary Figure 5). We do not know if the C2 element has evolved only in a subset of invertebrates (e.g. the ecdysozoa), or was already present in early metazoans and subsequently diverged in the vertebrate lineage. In any case, our observations raise the possibility that vertebrate Cic proteins are not subject to RTK regulation, although we cannot rule out that such regulation occurs through alternative regulatory motifs different from the C2 element. Clarification of this issue will require further molecular and developmental studies of Cic proteins in vertebrate systems.

Materials and methods

Drosophila strains and transgenic lines

The following stocks were used: cic^{1} (Jiménez *et al*, 2000); cic^{fetU6}, cic^{fetE11} (Goff *et al*, 2001); $Gal4^{T155}$, *UAS-λtop* (Queenan *et al*, 1997). Cic derivatives were expressed under the control of 5′ and 3′ genomic regulatory sequences present in the original *cic* rescue construct (Jiménez *et al*, 2000), and were assembled in p*CaSpeR4*. The different Cic constructs have the following amino-acid deletions: Cic^{mini} (82–474 and 598–1042), $Cic^{\Delta HMG}$ (386–582), $Cic^{miniNLS}$ (82–1042), $Cic^{\Delta C1}$ (1308–1355) and $Cic^{\Delta C2}$ (1052–1072). The $Cic^{miniNLS}$ product contains the SV40 NLS (PKKKRKV) inserted between residues 82 and 1042. All derivatives have a triple HA tag (YPYDVPDYA) inserted at position 1398.

P-element-mediated transformation was carried out using standard methods. In general, at least two independent insertions were examined for each construct. Strong $cic^{\Delta C2}$ lines were kept unbalanced selecting for transformant males in each generation. The effects of $Cic^{\Delta C2}$ were typically assayed using females carrying two $cic^{\Delta C2}$ insertions: one strong and one weak. The $cic^{\Delta C2}$, cic^{h1} and cic^{T1059D} lines (see Supplementary Figures 2 and 5) caused similar levels of embryonic lethality. Essentially the same results were also obtained with a Cic^{mini} derivative lacking the C2 motif (not shown).

Embryo and ovary analyses

Embryos and ovaries were fixed in 4% formaldehyde/PBS using standard methods. Devitellinization of embryos for subsequent staining with rhodamine–phalloidin (Sigma; 1:800 dilution) was carried out using 80% ethanol instead of methanol. Antibody and rhodamine–phalloidin stainings were performed according to standard procedures; detailed protocols are available on request. Immunodetection of HA-tagged Cic proteins was performed using monoclonal antibody 12CA5 (Roche) at 1:100 dilution. Mirr was detected using a rabbit polyclonal antibody (kindly provided by H McNeill) diluted 1:1000. Activated MAPK stainings were carried out using a monoclonal antibody that recognizes the diphosphorylated form of MAPK (Sigma; 1:1000 dilution). Signals were detected using appropriate secondary fluorochrome-conjugated antibodies (Molecular Probes, Amersham), and analyzed by confocal microscopy (Leica).

In situ hybridizations of embryos and ovaries were performed with digoxygenin-labeled (Roche) antisense RNA probes, using modifications of the protocol described by Tautz and Pfeifle (1989). Embryos were mounted in Permount and photographed under Normarski illumination.

Yeast two-hybrid assays

Bait and prey plasmids were made by subcloning the relevant protein coding sequences into the *pLex202* and *pJG4–5* vectors, respectively. Fragments generated by PCR and all insertion sites were sequenced to verify the accuracy of the final constructs. Yeast transformations and interactions assays were done as previously described (Paroush *et al*, 1994); interactions were detected using a *lexA-lacZ* reporter plasmid, *pSH18–34*.

In vitro binding and phosphorylation assays

Sequences encoding Cic^{4} and $Cic^{4\Delta C2}$ were inserted into the *pGEX-4T-3* vector. GST-Hairy and GST-Jun constructs have been described previously (Paroush *et al*, 1994; Caelles *et al*, 1997). Rolled coding sequences were subcloned into *pET17b*. Expression of GST fusion proteins in the *Escherichia coli* strain *BL21* and binding assays to ^{35}S-methionine-labeled Rolled and Luciferase proteins (prepared using the TNT system, Promega) were performed as described (Paroush *et al*, 1994; Jiménez *et al*, 1997). Phosphorylation reactions were carried out essentially as described (Caelles *et al*, 1997) by incubating the relevant GST fusions with either Erk or JNK immunoprecipitated from non- or TPA-stimulated HeLa cells and non- or LPS-stimulated mouse bone marrow-derived macrophages, respectively. Kinase immunoprecipitates were obtained using anti-Erk (sc-154) and anti-JNK (sc-474) antibodies (Santa Cruz Biotechnology).

Sequences

The Cic protein sequences from different species shown in Figure 1A have the following accession numbers: Q9U1H0 (*Drosophila melanogaster*); XP_395209 (*Apis mellifera*); CAD44099 (*Caenorhabditis elegans*); AAK73515 (*Homo sapiens*); AAH58665 (*Mus musculus*); CAF90910 (*Tetraodon nigroviridis*). The *Anopheles* Cic sequences are encoded in the genomic scaffold, AAAB01008879.

Supplementary data

Supplementary data are available at *The EMBO Journal* Online (http://www.embojournal.org).

Acknowledgements

We thank S González-Crespo, M Freeman, E Martín-Blanco, H McNeill, L Nilson, T Hsu, T Schüpbach, the Bloomington *Drosophila* Research Center, the Developmental Studies Hybridoma Bank and the *Drosophila* Genomics Resource Center for fly stocks and reagents. We are grateful to E Morán for help and encouragement during this work. We also thank L Bardia and M Pons for advice with the confocal analyses and S González-Crespo, D Ish-Horowicz, E Cinnamon and A Nieto for helpful discussions and critical comments on the manuscript. This work was supported by grants from the Spanish Ministry of Science and Education (BMC2002-01214 and BFU2005-02673 to GJ and BFU2004-02096 to CC), the Israel Science Foundation (501/04), the Israel Cancer Research Fund (project grant) and the Jan M and Eugenia Król Charitable Foundation to ZP. ZP is a Braun Lecturer. GJ is an ICREA Investigator.

References

Atkey MR, Lachance J-FB, Walczak M, Rebello T, Nilson LA (2006) Capicua regulates follicle cell fate in the *Drosophila* ovary through repression of *mirror*. *Development* **133:** 2115–2123

Biggs III WH, Zavitz KH, Dickson B, van der Straten A, Brunner D, Hafen E, Zipursky SL (1994) The *Drosophila rolled* locus encodes a MAP kinase required in the sevenless signal transduction pathway. *EMBO J* **13:** 1628–1635

Biggs III WH, Zipursky SL (1992) Primary structure, expression, and signal-dependent tyrosine phosphorylation of a *Drosophila* homolog of extracellular signal-regulated kinase. *Proc Natl Acad Sci USA* **89:** 6295–6299

Brönner G, Chu-LaGraff Q, Doe CQ, Cohen B, Weigel D, Taubert H, Jäckle H (1994) Sp1/egr-like zinc-finger protein required for endoderm specification and germ-layer formation in *Drosophila*. *Nature* **369:** 664–668

Brönner G, Jäckle H (1991) Control and function of terminal gap gene activity in the posterior pole region of the *Drosophila* embryo. *Mech Dev* **35:** 205–211

Brunner D, Oellers N, Szabad J, Biggs III WH, Zipursky SL, Hafen E (1994) A gain-of-function mutation in *Drosophila* MAP kinase activates multiple receptor tyrosine kinase signaling pathways. *Cell* **76:** 875–888

Caelles C, Gonzalez-Sancho JM, Muñoz A (1997) Nuclear hormone receptor antagonism with AP-1 by inhibition of the JNK pathway. *Genes Dev* **11:** 3351–3364

Casanova J (1990) Pattern formation under the control of the terminal system in the *Drosophila* embryo. *Development* **110:** 621–628

Cinnamon E, Gur-Wahnon D, Helman A, St Johnston D, Jiménez G, Paroush Z (2004) Capicua integrates input from two maternal systems in *Drosophila* terminal patterning. *EMBO J* **23:** 4571–4582

Duffy JB, Perrimon N (1994) The Torso pathway in *Drosophila*: lessons on receptor tyrosine kinase signaling and pattern formation. *Dev Biol* **166:** 380–395

Furriols M, Casanova J (2003) In and out of Torso RTK signalling. *EMBO J* **22:** 1947–1952

Goff DJ, Nilson LA, Morisato D (2001) Establishment of dorsal-ventral polarity of the *Drosophila* egg requires *capicua* action in ovarian follicle cells. *Development* **128:** 4553–4562

Greenwood S, Struhl G (1997) Different levels of Ras activity can specify distinct transcriptional and morphological consequences in early *Drosophila* embryos. *Development* **124:** 4879–4886

Hsu T, Bagni C, Sutherland JD, Kafatos FC (1996) The transcriptional factor CF2 is a mediator of EGF-R-activated dorsoventral patterning in *Drosophila* oogenesis. *Genes Dev* **10:** 1411–1421

Hsu T, McRackan D, Vincent TS, Gert de Couet H (2001) *Drosophila* Pin1 prolyl isomerase Dodo is a MAP kinase signal responder during oogenesis. *Nat Cell Biol* **3:** 538–543

Ishitani T, Ninomiya-Tsuji J, Nagai S, Nishita M, Meneghini M, Baker N, Waterman M, Bowerman B, Clevers H, Shibuya H, Matsumoto K (1999) The TAK1-NLK-MAPK-related pathway antagonizes signalling between β-catenin and transcription factor TCF. *Nature* **399:** 798–802

Janody F, Sturny R, Schaeffer V, Azou Y, Dostatni N (2001) Two distinct domains of Bicoid mediate its transcriptional downregulation by the Torso pathway. *Development* **128:** 2281–2290

Jiménez G, Guichet A, Ephrussi A, Casanova J (2000) Relief of gene repression by Torso RTK signaling: role of capicua in *Drosophila* terminal and dorsoventral patterning. *Genes Dev* **14:** 224–231

Jiménez G, Paroush Z, Ish-Horowicz D (1997) Groucho acts as a corepressor for a subset of negative regulators, including Hairy and Engrailed. *Genes Dev* **11:** 3072–3082

Jordan KC, Clegg NJ, Blasi JA, Morimoto AM, Sen J, Stein D, McNeill H, Deng WM, Tworoger M, Ruohola-Baker H (2000) The homeobox gene *mirror* links EGF signalling to embryonic dorso-ventral axis formation through Notch activation. *Nat Genet* **24:** 429–433

Kalderon D, Roberts BL, Richardson WD, Smith AE (1984) A short amino acid sequence able to specify nuclear location. *Cell* **39:** 499–509

Liaw GJ, Rudolph KM, Huang JD, Dubnicoff T, Courey AJ, Lengyel JA (1995) The *torso* response element binds GAGA and NTF-1/Elf-1, and regulates *tailless* by relief of repression. *Genes Dev* **9:** 3163–3176

Mantrova EY, Hsu T (1998) Down-regulation of transcription factor CF2 by *Drosophila* Ras/MAP kinase signaling in oogenesis: cytoplasmic retention and degradation. *Genes Dev* **12:** 1166–1175

Murphy LO, Smith S, Chen R-H, Fingar DC, Blenis J (2002) Molecular interpretation of ERK signal duration by immediate early gene products. *Nat Cell Biol* **4:** 556–564

Paroush Z, Finley Jr RL, Kidd T, Wainwright SM, Ingham PW, Brent R, Ish-Horowicz D (1994) Groucho is required for *Drosophila* neurogenesis, segmentation, and sex determination and interacts directly with hairy-related bHLH proteins. *Cell* **79:** 805–815

Paroush Z, Wainwright SM, Ish-Horowicz D (1997) Torso signalling regulates terminal patterning in *Drosophila* by antagonising Groucho-mediated repression. *Development* **124:** 3827–3834

Peri F, Bokel C, Roth S (1999) Local Gurken signaling and dynamic MAPK activation during *Drosophila* oogenesis. *Mech Dev* **81:** 75–88

Pignoni F, Baldarelli RM, Steingrimsson E, Diaz RJ, Patapoutian A, Merriam JR, Lengyel JA (1990) The *Drosophila* gene *tailless* is expressed at the embryonic termini and is a member of the steroid receptor superfamily. *Cell* **62:** 151–163

Pignoni F, Steingrímsson E, Lengyel JA (1992) *bicoid* and the terminal system activate *tailless* expression in the early *Drosophila* embryo. *Development* **115:** 239–251

Queenan AM, Ghabrial A, Schupbach T (1997) Ectopic activation of *torpedo/Egfr*, a *Drosophila* receptor tyrosine kinase, dorsalizes both the eggshell and the embryo. *Development* **124:** 3871–3880

Ray RP, Schüpbach T (1996) Intercellular signaling and the polarization of body axes during *Drosophila* oogenesis. *Genes Dev* **10:** 1711–1723

Reuter R, Leptin M (1994) Interacting functions of *snail*, *twist* and *huckebein* during the early development of germ layers in *Drosophila*. *Development* **120:** 1137–1150

Roch F, Jiménez G, Casanova J (2002) EGFR signalling inhibits Capicua-dependent repression during specification of *Drosophila* wing veins. *Development* **129:** 993–1002

Rommel C, Hafen E (1998) Ras—a versatile cellular switch. *Curr Opin Genet Dev* **8:** 412–418

Ronchi E, Treisman J, Dostatni N, Struhl G, Desplan C (1993) Down-regulation of the *Drosophila* morphogen Bicoid by the Torso receptor-mediated signal transduction cascade. *Cell* **74:** 347–355

Ruohola-Baker H, Grell E, Chou TB, Baker D, Jan LY, Jan YN (1993) Spatially localized *rhomboid* is required for establishment of the dorsal-ventral axis in *Drosophila* oogenesis. *Cell* **73:** 953–965

Rusch J, Levine M (1996) Threshold responses to the dorsal regulatory gradient and the subdivision of primary tissue territories in the *Drosophila* embryo. *Curr Opin Genet Dev* **6:** 416–423

Schüpbach T (1987) Germ line and soma cooperate during oogenesis to establish the dorsoventral pattern of egg shell and embryo in *Drosophila melanogaster*. *Cell* **49:** 699–707

Sen J, Goltz JS, Stevens L, Stein D (1998) Spatially restricted expression of *pipe* in the *Drosophila* egg chamber defines embryonic dorsal-ventral polarity. *Cell* **95:** 471–481

Simon MA (2000) Receptor tyrosine kinases: specific outcomes from general signals. *Cell* **103:** 13–15

Tan PB, Kim SK (1999) Signaling specificity: the RTK/RAS/MAP kinase pathway in metazoans. *Trends Genet* **15:** 145–149

Tanoue T, Adachi M, Moriguchi T, Nishida E (2000) A conserved docking motif in MAP kinases common to substrates, activators and regulators. *Nat Cell Biol* **2:** 110–116

Tanoue T, Nishida E (2003) Molecular recognitions in the MAP kinase cascades. *Cell Signal* **15:** 455–462

Tautz D, Pfeifle C (1989) A non-radioactive *in situ* hybridization method for the localization of specific RNAs in *Drosophila* embryos reveals translational control of the segmentation gene *hunchback*. *Chromosoma* **98:** 81–85

Wasserman JD, Freeman M (1998) An autoregulatory cascade of EGF receptor signaling patterns the *Drosophila* egg. *Cell* **95:** 355–364

Zhao D, Woolner S, Bownes M (2000) The Mirror transcription factor links signalling pathways in *Drosophila* oogenesis. *Dev Genes Evol* **210:** 449–457